Scientific Research Publishing

Open Journal of Applied Sciences, 2019, 9, 181-197
http://www.scirp.org/journal/ojapps
ISSN Online: 2165-3925
ISSN Print: 2165-3917

Design and Analysis of MEMS Based Aluminum Nitride (AlN), Lithium Niobate ($LiNbO_3$) and Zinc Oxide (ZnO) Cantilever with Different Substrate Materials for Piezoelectric Vibration Energy Harvesters Using COMSOL Multiphysics Software

Ahmad M. Alsaad[1*], Ahmad A. Ahmad[1,2], Qais M. Al-Bataineh[1], Nermeen S. Daoud[1], Mais H. Khazaleh[1]

[1]Department of Physical Sciences, Jordan University of Science and Technology, Irbid, Jordan
[2]Department of Physics, Faculty of Sciences, University of Hafr Al-Batin, Hafr Al-Batin, Saudi Arabia
Email: *alsaad11@just.edu.jo

How to cite this paper: Alsaad, A.M., Ahmad, A.A., Al-Bataineh, Q.M., Daoud, N.S. and Khazaleh, M.H. (2019) Design and Analysis of MEMS Based Aluminum Nitride (AlN), Lithium Niobate ($LiNbO_3$) and Zinc Oxide (ZnO) Cantilever with Different Substrate Materials for Piezoelectric Vibration Energy Harvesters Using COMSOL Multiphysics Software. *Open Journal of Applied Sciences*, **9**, 181-197.
https://doi.org/10.4236/ojapps.2019.94016

Received: March 12, 2019
Accepted: April 16, 2019
Published: April 19, 2019

Abstract

Interest in energy harvesters has grown rapidly over the last decade. The cantilever shaped piezoelectric energy harvesting beam is one of the most employed designs, due to its simplicity and flexibility for further performance enhancement. The research effort in the MEMS Piezoelectric vibration energy harvester designed using three types of cantilever materials, Lithium Niobate ($LiNbO_3$), Aluminum Nitride (AlN) and Zinc Oxide (ZnO) with different substrate materials: aluminum, steel and silicon using COMSOL Multiphysics package were designed and analyzed. Voltage, mechanical power and electrical power versus frequency for different cantilever materials and substrates were modeled and simulated using Finite element method (FEM). The resonant frequencies of the $LiNbO_3$/Al, AlN/Al and ZnO/Al systems were found to be 187.5 Hz, 279.5 Hz and 173.5 Hz, respectively. We found that ZnO/Al system yields optimum voltage and electrical power values of 8.2 V and 2.8 mW, respectively. For ZnO cantilever on aluminum, steel and silicon substrates, we found the resonant frequencies to be 173.5 Hz, 170 Hz and 175 Hz, respectively. Interestingly, ZnO/steel yields optimal voltage and electrical power values of 9.83 V and 4.02 mW, respectively. Furthermore, all systems were studied at different differentiate frequencies. We found that voltage and electrical power have increased as the acceleration has increased.

Keywords

MEMS, Piezoelectric, Energy Harvester, Cantilever, Lithium Niobate ($LiNbO_3$), Aluminum Nitride (AlN), Zinc Oxide (ZnO), Aluminium Substrate, Steel Substrate, Silicon Substrate, COMSOL, Finite Element Method

1. Introduction

Micro-electro mechanical system (MEMS) devices have a wide area of applications as pressure sensors, accelerometers, gyroscopes etc. [1]. In recent decades, energy harvesting from ambient vibrations of natural environments, such as air flows and human motions, which are obtainable universally and permanently, has attracted much attention of many researches [2]. The investigations in vibration-based energy harvester using piezoelectric transducers have been attracting intensive attention in the research sector of sustainable energy [3]. Piezoelectric energy harvesters (PEH) have the distinctive capacity to convert ambient vibration energy from the surrounding environment into electrical power [4] [5] [6]. A typical PEH system usually consists of two parts: a mechanical structure and an energy harvesting circuit. The coupling between these two parts and the multidisciplinary nature of this field lead to a substantial challenge in modeling PEH system [7]. Piezoelectric materials are widely used in vibration energy harvesters (VEH) as mechanical-to-electrical transducers due to their relatively high power density [8], scalability and compatibility with conventional integrated circuit technologies [9] [10] [11].

Simulation modeling solves real-world problems safely and efficiently. It provides an important method of analysis which is easily verified, communicated, and understood. Across industries and disciplines, simulation modeling provides cherished solutions by giving clear insights into complex systems. Mathematical modeling and simulations have been used to predict the optimized properties and to evaluate the performance of systems similar to our proposed system [12] [13]. COMSOL Multiphysics® (known as FEMLAB before 2005) is a software package designed to investigate a wide range of physical phenomena of different systems using finite element method [14].

AlN, $LiNbO_3$ and ZnO have extensive applications in several fields because of their outstanding piezoelectric and pyroelectric properties, as well as, elastic- and electro-optic effects [15] [16] [17]. Several previous works have studied PEH based on AlN [18] [19], $LiNbO_3$ [20] and ZnO [21] [22] [23] Cantilevers due to their significant contributions in the modern technology of MEMS devices.

In this work, PEH systems were modelled by COMSOL Multiphysics software using AlN, $LiNbO_3$ and ZnO Cantilevers assembled on Aluminum, Steel and Silicon substrates. The main objective of this work is to reveal the most efficient cantilever/substrate combination that has the optimized electrical and piezoelec-

tric properties. Particularly, we investigate the behavior of the output voltage, power (mechanical and electrical) as well as piezoelectric response a function of frequency and acceleration.

2. Mathematical Model for Piezoelectric Beam

Cantilever structure is the most common structure used for piezoelectric energy harvester [24]. Cantilever can be defined as a structure with one end fixed and other end free to vibrate, made up of one or more layer of piezoelectric material bonded to an elastic metal in order to increase the sensitivity of the structure and reduce the brittleness of the piezoelectric layer [25].

Electric charge is generated when mechanical stress is applied on a piezoelectric material. IEEE standard on piezoelectricity has given different form of piezoelectric constitutive equations. Strain-charge form has been used for cantilever structure and the equations are:

$$S = s^E T + d_{ij} \overline{E} \tag{1}$$

$$D = d_{ij} T + \varepsilon^{\mathrm{T}} \overline{E} \tag{2}$$

where: S is mechanical strain, s^E is elastic compliance tensor (Pa^{-1}), T is mechanical stress vector ($\mathrm{N{\cdot}m}^{-2}$), $\overline{E}$ is electric field vector ($\mathrm{V{\cdot}m}^{-1}$), D is electrical displacement ($\mathrm{C{\cdot}m}^{-2}$), ε^{T} is dielectric permittivity tensor ($\mathrm{F{\cdot}m}^{-1}$) and d_{ij} is electro-mechanical coupling factor ($\mathrm{C{\cdot}N}^{-1}$), where i is the polarization direction and j is the strain direction.

There are two approaches used in the design of a piezoelectric harvester: longitudinal and transversal approaches. The first is the longitudinal mode (d_{31}) where the polarization of the beam is laterally developed in the deposited film. The frequently used is the transversal mode (d_{33}) where the polarization of the beam is perpendicular to the deposited film.

The resonant frequency is the most important parameter of a vibration energy harvesting device. It is calculated by using the given equation [26]:

$$f_n = \frac{v_n^2}{2\pi} \frac{1}{L^2} \sqrt{\frac{D_p}{m}} \tag{3}$$

where: $v_n = 1.875$ for first mode, m is the mass per unit area and D_p is the bending modulus which is a function of Young's modulus and thickness of the substrate and expressed by:

$$D_p = \frac{E_P^2 t_p^4 + E_s^2 t_s^4 + 2E_S E_P t_p t_s \left(2t_p^2 + 2t_s^2 + 3t_p t_s\right)}{12\left(E_P t_p + E_S t_s\right)} \tag{4}$$

Hence the variation of resonant frequency is

$$f_n \propto \frac{1}{L^2} \sqrt{t_p} \sqrt{t_s} \tag{5}$$

where: L: length of the harvester, t_p : thickness of the piezoelectric layer and t_s : thickness of the substrate layer. Cantilever oscillates when placed in vibrating

environment. The oscillations attain the optimum peak as the vibration frequency of the environment matches the resonance frequency of the cantilever structure, and damps out significantly for all other frequencies. The frequency of the source vibrations present in the environment mostly has frequencies in the range of 50 - 200 Hz. The proof mass lowers the resonance frequency of the cantilever by order of few Hz, which is normally the order of frequency of vibration present in the nature. Proof mass also increases the amount of deflection, hence increasing the stress at the fixed end due to which charge is generated in the cantilever structure. Electrical output voltage is highest when stress is maximum, which is occurs at the resonance frequency [25].

3. COMSOL Multiphysics Simulation

To simulate the piezoelectric vibration energy harvester using COMSOL Multiphysics, the piezoelectric devices Multiphysics interface and electrical circuit have to be chosen. Solid mechanics and electrostatics are combined within the piezoelectric devices Multiphysics interface with the constitutive relationships required to model the piezoelectric device.

3.1. Geometric Modeling

2D geometry is considered for the simulations. The cantilever contains aluminum, steel or silicon thin substrate of 40 μm thickness (**Table 1** displays the properties of substrate materials) coated by two layers of AlN, $LiNbO_3$ or ZnO of 60 μm in thickness. The dimensions of the cantilever is (20 × 14) mm, with a mass of aluminum block of dimension (4 × 14 × 1.7) mm on the vibrating end of the cantilever, as shown in **Figure 1**.

3.2. Boundary Settings

The base of our simulated piezoelectric vibration energy harvester is designed to have one end fixed and the other end is free to vibrate with a mass of aluminum is attached to it. The upper end of the cantilever is taken to be free in response to the applied force. The upper surface of the AlN, $LiNbO_3$ or ZnO is taken to be ground and the lower surface is connected to external circuit.

3.3. Meshing

Before starting simulation, the piezoelectric vibration energy harvester has be divided into small areas; each is called a "mesh". In this work, the mesh was

Table 1. The properties of substrate materials.

Substrate Materials	Density (kg/m^3)	Young's modulus (10^9 Pa)	Poisson's ratio
Aluminum	2700	70	0.33
Steel	7850	200	0.30
Silicon	2329	170	0.28

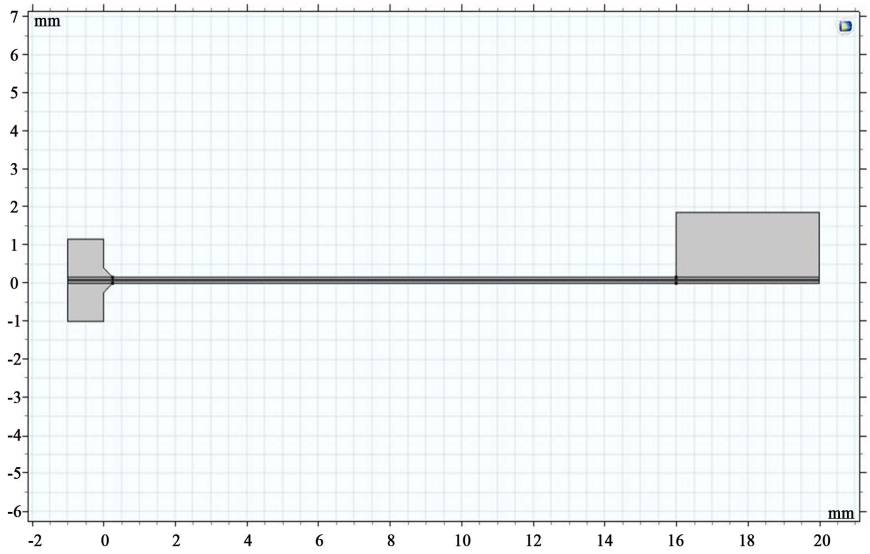

Figure 1. The geometry of piezoelectric vibration energy harvester.

taken to be "Free triangular" with element size parameter ranging between 0.002 and 0.02. **Figure 2** illustrates the obtained mesh for a piezoelectric vibration energy harvester.

3.4. Simulation Results

The mass attached to the vibrating end of the piezoelectric vibration energy harvester is simulated to obtain the required mass needed to reach the resonant frequency that yields the maximum voltage, as displayed in **Figure 3(a)**. **Figure 3(b)** demonstrates the obtained electric force at resonant frequency. We found that the resonant frequency of AlN/Al, $LiNbO_3$/Al and ZnO/Al are 279.5 Hz, 187.5 Hz and 173.5 Hz, respectively.

4. Results and Discussions

In this section, we describe and interpret our results on the piezoelectric vibration energy harvester output voltage and power (mechanical and electrical) behavior of the $LiNbO_3$, AlN and ZnO cantilevers assembled on different types of substrates (aluminum, steel and silicon) as functions of frequency and acceleration responses.

4.1. $LiNbO_3$, AlN and ZnO Cantilevers with Aluminum Substrate

4.1.1. Frequency Response

Figure 4 shows the measured voltage of $LiNbO_3$, AlN and ZnO cantilevers assembled on Al substrate as a function of frequency, with a host acceleration of 1 g (g is the acceleration due to gravity) and load resistance of 12 kΩ. As can be seen from **Figure 4**, the resonant frequency demonstrated by $LiNbO_3$, AlN and ZnO cantilevers is 187.5 Hz, 279.5 Hz and 173.5 Hz, respectively. Figure 4 clearly shows that ZnO cantilever exhibits the maximum voltage value of 8.2 V at a resonant frequency of 173.5 Hz. **Figure 5** and **Figure 6** illustrate the calculated

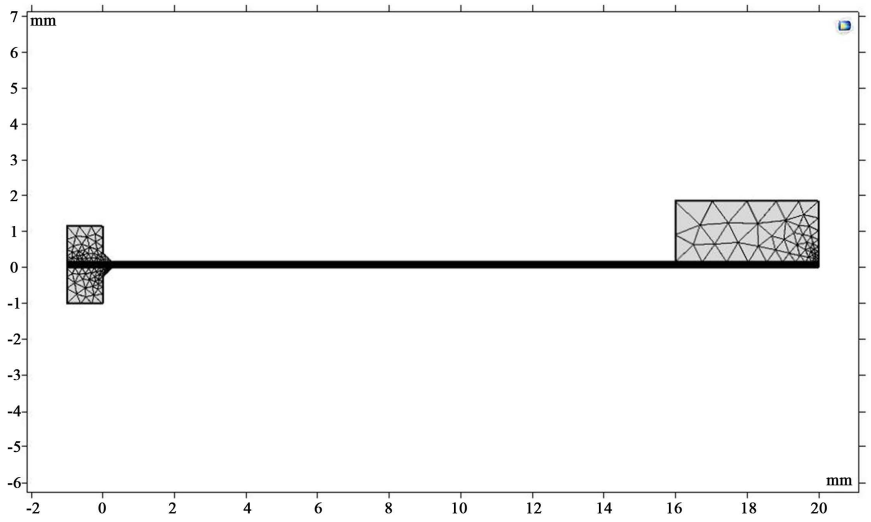

Figure 2. Piezoelectric vibration energy harvester mesh.

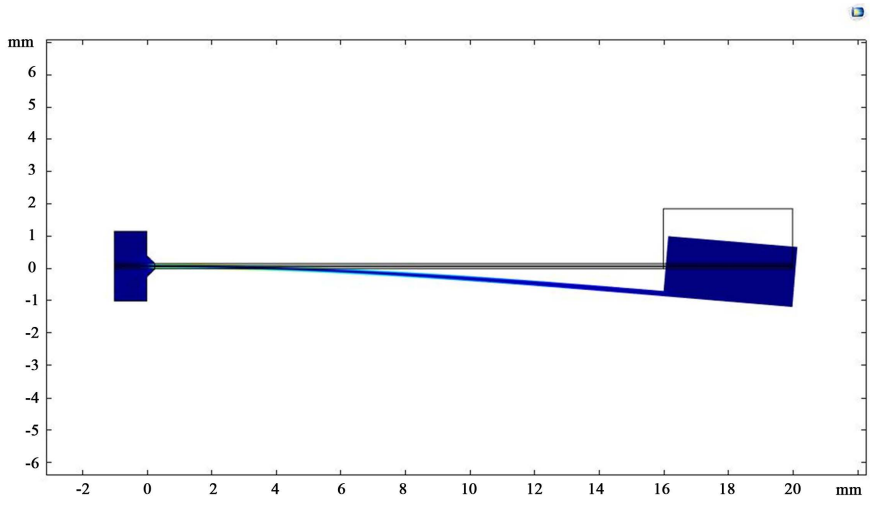

(a)

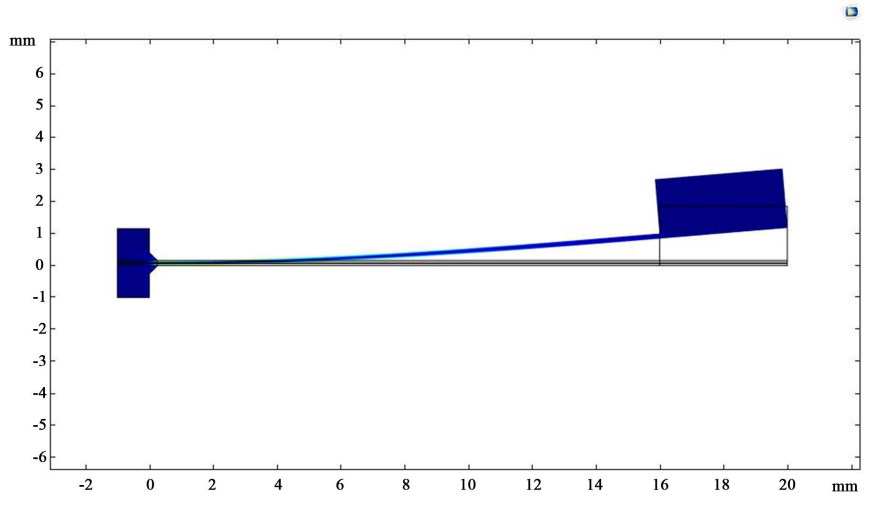

(b)

Figure 3. The simulation results of strain for piezoelectric vibration energy harvester.

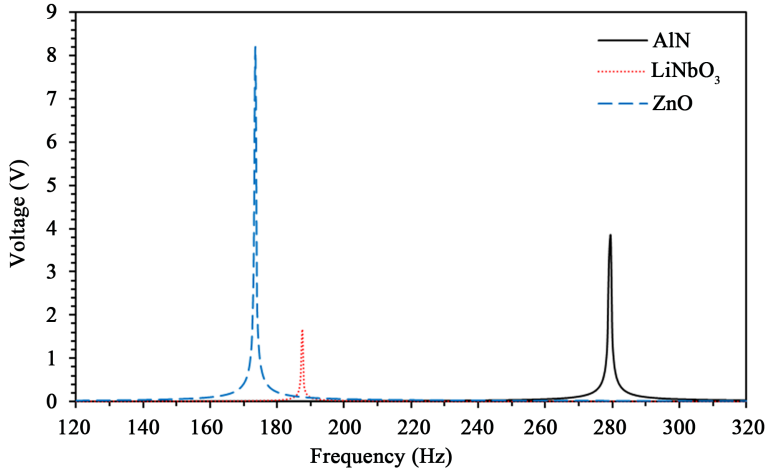

Figure 4. Measured voltage (V) versus frequency (Hz) for $LiNbO_3$, AlN and ZnO cantilevers.

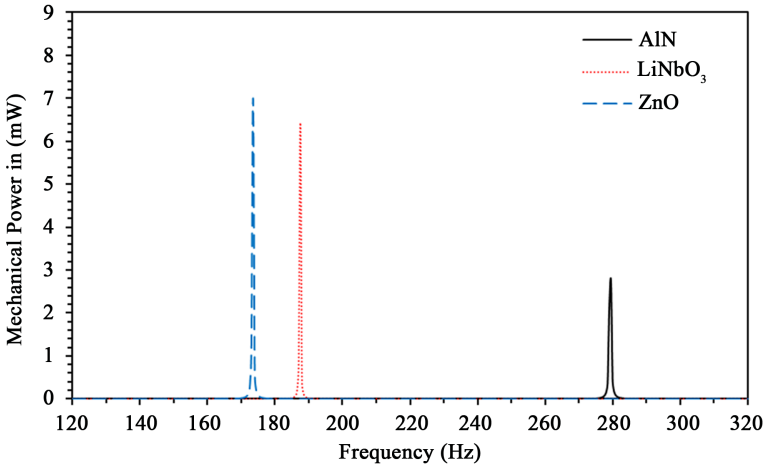

Figure 5. Measured Mechanical power in (mW) versus frequency (Hz) for $LiNbO_3$, AlN and ZnO cantilevers.

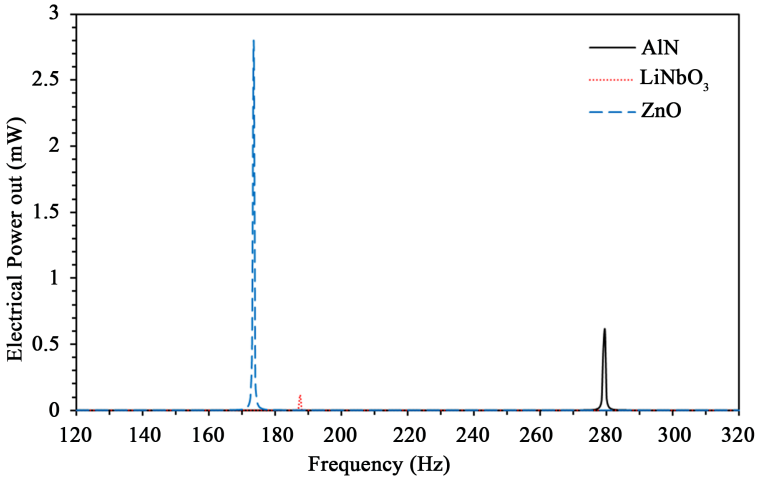

Figure 6. Measured Electrical power out (mW) versus frequency (Hz) for $LiNbO_3$, AlN and ZnO cantilevers.

mechanical power input and electrical output power of the piezoelectric vibration energy harvester designed using $LiNbO_3$, AlN and ZnO cantilevers. Obviously, the ZnO cantilever attains the maximum electrical power output of 2.8 mW at a resonant frequency of 173.5 Hz.

The ZnO/Al cantilever attains the maximum voltage and output electrical power at the resonant frequency in comparison with the other two investigated systems since it exhibits attractive exceptionally high piezoelectric properties. Piezoelectric properties of materials depend on three main parameters: structure, piezoelectric coefficient (e_{13} and e_{33}) and dipole moment. The ZnO and AlN both adopt a wurtzite structure with a space group of (C_{6v}^4-$P6_3mc$) in their equilibrium phase, thus, exhibiting interesting piezoelectric properties, high voltage and output electrical power at the resonant frequency. On the other hand, $LiNbO_3$ exhibits a trigonal structure with a space group($R3c$), as a result, it attains the minimum voltage and output electrical power at the resonant frequency. We found that AlN piezoelectric coefficients ($e_{13} = -0.580\ \mathrm{C\cdot m^{-2}}$ and $e_{33} = 1.550\ \mathrm{C\cdot m^{-2}}$), respectively that are close to those of ZnO ($e_{13} = -0.567\ \mathrm{C\cdot m^{-2}}$ and $e_{33} = 1.320\ \mathrm{C\cdot m^{-2}}$). However, the dipole moment of ZnO is ($\mu = 0.345$ Debey) that is much larger than that of AlN ($\mu = 0.096$ Debey), as shown in Table 2. This is because Zn^{2+} cations and O^{2-} anions change their position under a stress (force) in a nonhomogenous way. Thus an induced net polarization develops in the material. Moreover, electric dipoles which created by the non-homogenous distribution of Zn^{2+} cations and O^{2-} anions would be sustained, as long as external stress is applied [27] [28]. The induced polarization caused by the strain at the ZnO/Al interface is large due to the lattice mismatch between ZnO and Al substrate.

The AlN, and its related alloys are wide (direct) band gap semiconductors with high thermal and mechanical stability. They have attracted great attention for the fabrication of optoelectronic devices operating in the visible and ultraviolet regions at high power and under harsh environmental conditions. The determination of strains at the nanoscale is essential for the development of new electronic devices. The wurtzite hexagonal phase is energetically more stable for AlN and its alloys. This crystalline structure is non-centrosymmetric with a

Table 2. Comparative parameters for ZnO, AlN and $LiNbO_3$ cantilevers.

	ZnO	AlN	$LiNbO_3$
Structure	Wurtzite	Wurtzite	Trigonal
Space Group	C_{6v}^4-$P6_3mc$	C_{6v}^4-$P6_3mc$	R_3c
e_{13} ($C\cdot m^{-2}$)	−0.567	−0.580	0.194
e_{33} ($C\cdot m^{-2}$)	1.320	1.550	1.309
Young's modulus (GPa)	210 [29]	344 [30]	170 [31]
Dipole moment μ (Debey)	0.345 [32]	0.096 [33]	4.40 [34]

singular polar axis causing the formation of anelectric dipole in the unit cell due to the lack of coincidence of the centre of mass of the negative charge in the N tetrahedrons and the positive charge of the Al atom. The dipolegives rise to a spontaneous polarization. Moreover, in the presence of strain, apiezoelectric polarization is created at the AlN/Al interface due to the lattice mismatch between AlN and the Al substrates that can create fields in the MV/cm range. However, the lattice mismatch in ZnO/Al cantilevers is much larger than lattice mismatch in AlN/Al cantilevers.

4.1.2. Acceleration Response

Figure 7 displays the calculated voltage of $LiNbO_3$, AlN and ZnO cantilevers as a function of host acceleration calculated specifically at the resonant frequency of each of the investigated cantilevers and by keeping the load resistance fixed at 12 kΩ for all cases. Our results indicate that the voltage of the piezoelectric vibration energy harvester increases linearly as the host acceleration increases from 0.25g - 2 g, in excellent agreement with the findings of E. K. Reilly *et al.* study [35]. In addition, our results clearly demonstrate that ZnO cantilever exhibits larger voltage values than those attained by $LiNbO_3$ and AlN cantilevers.

Figure 8 and Figure 9 illustrate the calculated mechanical input power and the obtained electrical power output of the piezoelectric vibration energy harvester of the $LiNbO_3$, ZnO and AlN cantilevers. Apparently, the ZnO cantilever sustains the best electrical power output at the 173.5 Hz resonant frequency.

Inspecting the obtained results carefully indicate that among the three different cantilevers investigated, ZnO cantilevers yields better voltage and electrical output power. Now, we turn our attention to focus on investigating the electrical properties of ZnO cantilevers assembled on three different substrates, namely, aluminum, steel and silicon substrates.

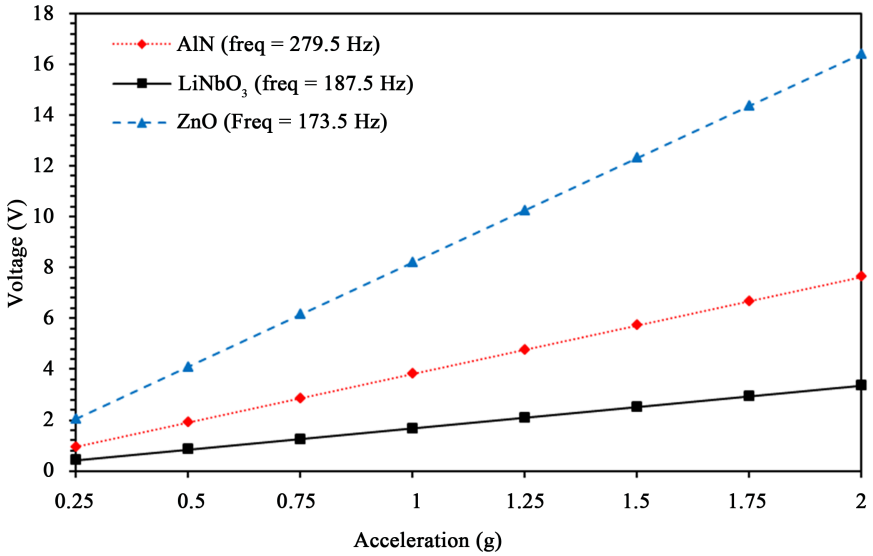

Figure 7. Calculated voltage (V) versus acceleration (g) for $LiNbO_3$, AlN and ZnO cantilevers at resonant frequency.

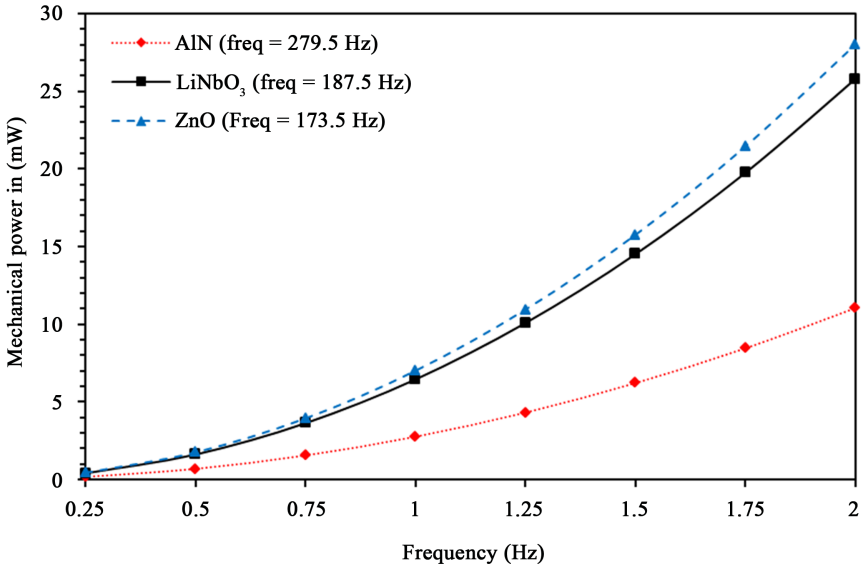

Figure 8. Calculated mechanical power input (mW) versus acceleration (g) of $LiNbO_3$, AlN and ZnO cantilevers at resonant frequency.

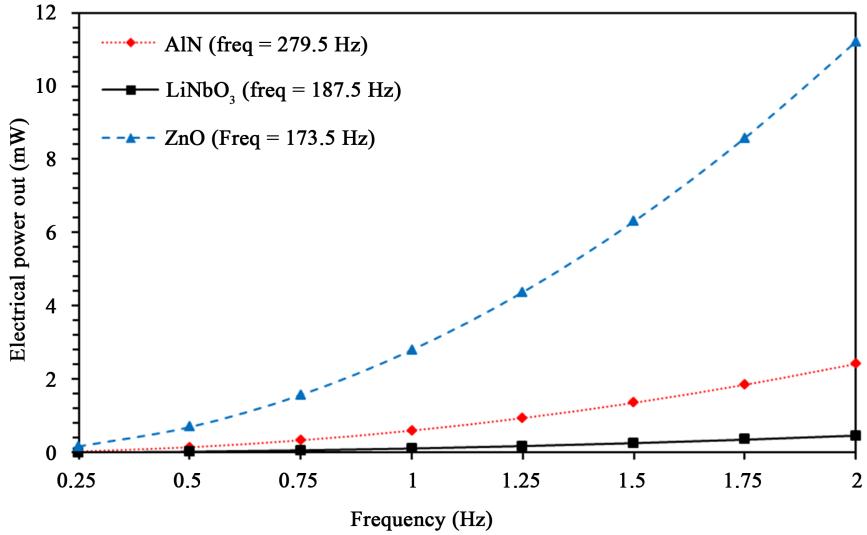

Figure 9. Calculated electrical power output (mW) versus acceleration (g) for $LiNbO_3$, AlN and ZnO cantilevers at resonant frequency.

4.2. ZnO Cantilevers with Aluminum, Steel and Silicon Substrates

4.2.1. Frequency Response

Figure 10 illustrates the calculated voltage of ZnO cantilevers assembled on aluminum, steel and silicon substrates as a function of frequency keeping the host acceleration fixed at 1 g and a predetermined load resistance of 12 kΩ. As can be clearly seen from **Figure 10**, the fundamental resonant frequency of the ZnO cantilevers assembled on aluminum, steel and silicon substrates was approximately 173.5 Hz, 170.0 Hz and 175 Hz, respectively, which is in the vicinity of the resonant frequency used in the experimental work of C.T. Pan *et al.* for ZnO cantilever on PET substrate [36]. Furthermore, ZnO cantilever assembled

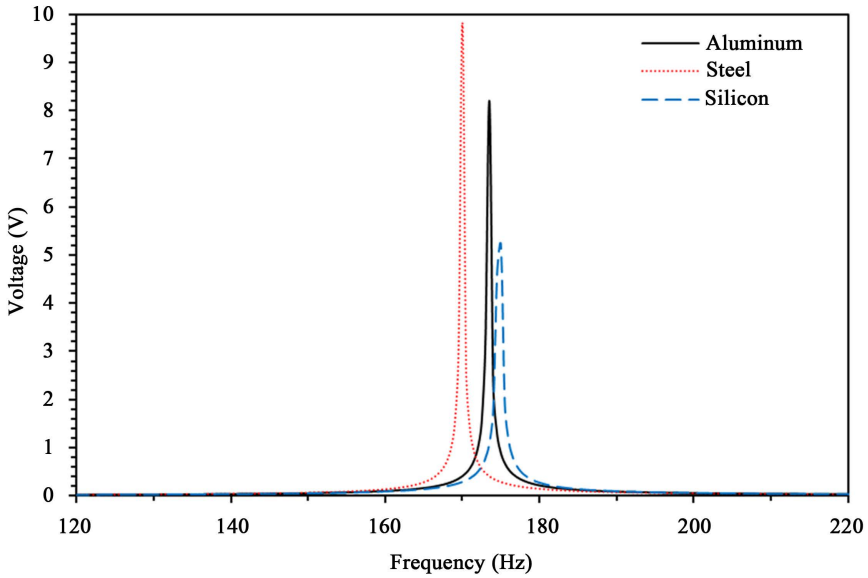

Figure 10. Calculated voltage versus frequency of ZnO cantilever assembled on aluminum, steel, and silicon substrates.

on steel substrate yields 9.83 V at the resonant frequency. This value is better than the ones obtained using ZnO cantilever assembled on aluminum and silicon substrates.

Figure 11 and **Figure 12** demonstrate the mechanical power input and the calculated electrical power output of the piezoelectric vibration energy harvester designed using ZnO cantilevers assembled on aluminum, steel and silicon substrates. **Figure 12** indicates that ZnO cantilevers assembled on steel substrates yields 4.02 of electrical power at resonant frequency 173.5 Hz larger than the electrical output power yielded using ZnO cantilevers assembled on aluminum and silicon substrates.

4.2.2. Acceleration Response

Figure 13 illustrates the calculated voltage of ZnO cantilevers assembled on aluminum, steel and silicon substrates as a function of host acceleration keeping the resonant frequency fixed at a predetermined value and using a constant value of load resistance of 12 kΩ for the three cases. As can be clearly seen from **Figure 13**, The voltage increases linearly as the host acceleration is increased gradually from 0.25 g - 2 g. Apparently, ZnO cantilever assembled on steel substrate yields an optimum value of voltage of approximately 20 V at a resonant frequency of 170 Hz. Whereas ZnO cantilever assembled on aluminum and silicon substrates yields a voltage of 16.4 V, 10.4 V at a resonant frequency of 173.5 Hz, 175 Hz, respectively.

Figure 14 and **Figure 15** illustrate the mechanical power input and the calculated electrical power output of the ZnO cantilever assembled on aluminum, steel, and silicon substrates. As can be seen from **Figure 15**, the ZnO cantilever assembled on steel substrates yields the maximum electrical power value of approximately 41 mW at a resonant frequency of 170 Hz.

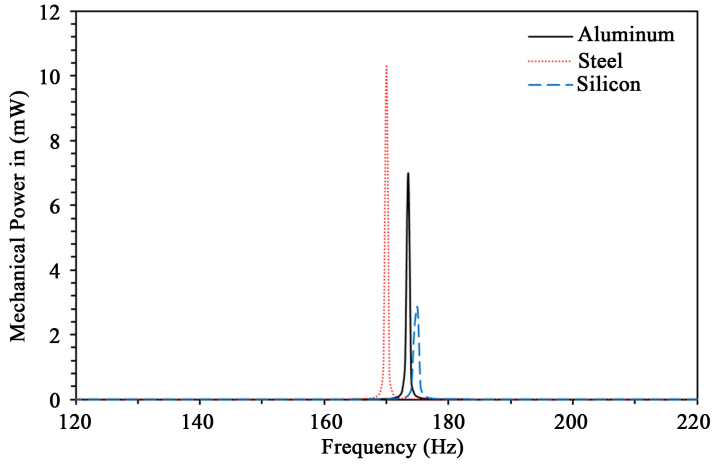

Figure 11. Mechanical power input versus frequency of ZnO cantilever assembled on aluminum, steel, and silicon substrates.

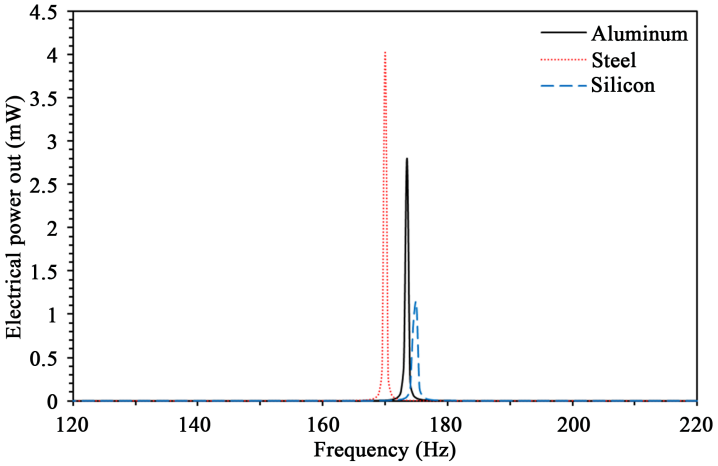

Figure 12. Calculated electrical power output versus frequency of ZnO cantilever assembled on aluminum, steel, and silicon substrates.

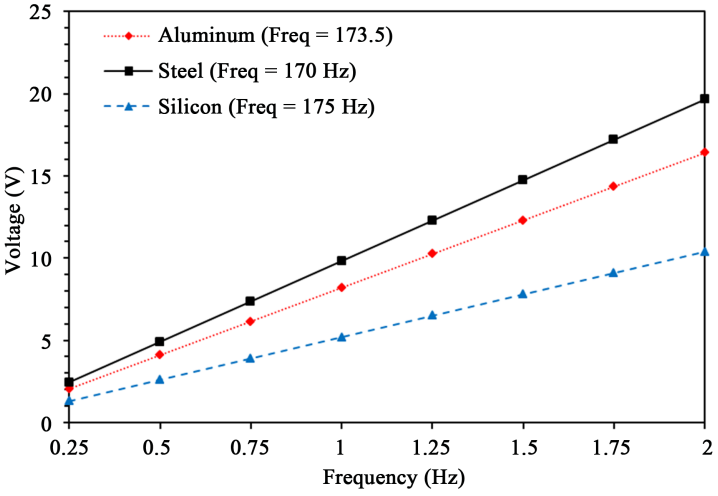

Figure 13. Calculated voltage versus host acceleration (g) of ZnO cantilever assembled on aluminum, steel, and silicon substrates at fixed predetermined resonant frequency.

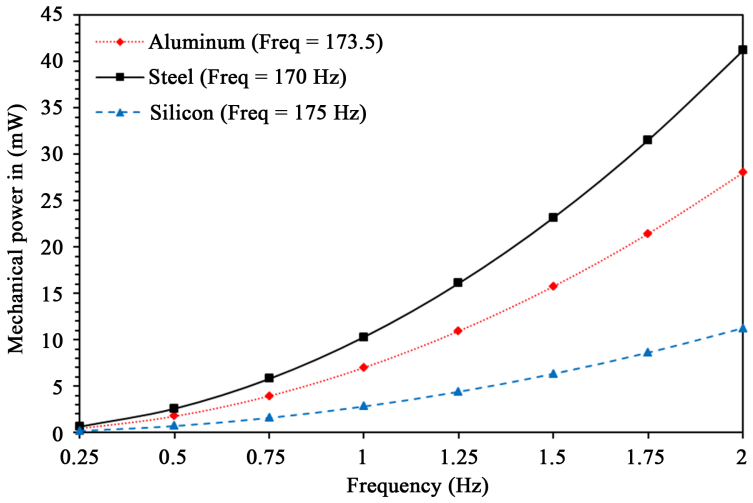

Figure 14. Mechanical power input versus host acceleration of ZnO cantilever assembled on aluminum, steel, and silicon substrates at a predetermined fixed resonant frequency.

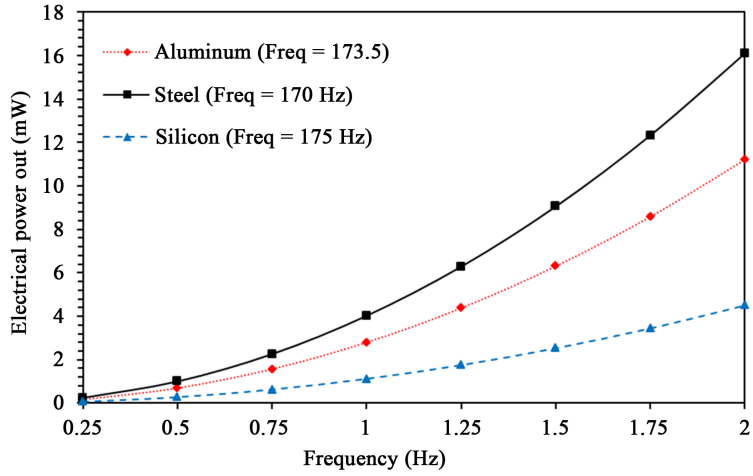

Figure 15. Calculated electrical power output versus host acceleration of ZnO cantilever assembled on aluminum, steel, and silicon substrates at a predetermined fixed resonant frequency.

4.3. All Cantilever Materials with All Substrate Materials

Table 3 and Table 4 summarize the voltage and electrical power output of the three cantilever materials (ZnO, $LiNbO_3$ and AlN) assembled on aluminum, steel and silicon substrates calculated at a predetermined fixed resonant frequency. The tables summarize our main findings described in details in the text.

5. Conclusions

In Summary, $LiNbO_3$, AlN and zinc oxide (ZnO) cantilever materials assembled on aluminum, steel and silicon substrates have been investigated using COMSOL Multiphysics based on Finite Element Method (FEM).Voltage, mechanical power input and electrical power output versus frequency for each system were calculated and found to change linearly with the frequency.

Table 3. The voltage yielded at the predetermined fixed resonant frequency of ZnO, $LiNbO_3$, AlN cantilevers assembled on aluminum, steel and silicon substrates.

	ZnO	$LiNbO_3$	AlN
Aluminum	173.5 Hz, 8.20 V	187.5 Hz, 1.67 V	279.5 Hz, 3.80 V
Steel	170.0 Hz, 9.82 V	183.5 Hz, 1.49 V	272.0 Hz, 4.86 V
Silicon	175.0 Hz, 5.19 V	189.0 Hz, 1.00 V	281.0 Hz, 4.4 V

Table 4. The electrical power output yielded at the predetermined fixed resonant frequency of ZnO, $LiNbO_3$, AlN cantilevers assembled on aluminum, steel and silicon substrates.

	ZnO	$LiNbO_3$	AlN
Aluminum	173.5 Hz, 2.80 mW	187.5 Hz, 0.12 mW	279.5 Hz, 0.61 mW
Steel	170.0 Hz, 4.02 mW	183.5 Hz, 0.10 mW	272.0 Hz, 0.92 mW
Silicon	175.0 Hz, 1.12 mW	189.0 Hz, 0.04 mW	281.0 Hz, 0.81 mW

The resonant frequency of $LiNbO_3$, AlN and ZnO cantilevers are found to be 187.5 Hz, 279.5 Hz and 173.5 Hz, respectively. Interestingly, ZnO cantilever yields the maximum voltage and electrical power values of 8.2 V and 2.8 mW, respectively when examined at resonance frequency of 173.5 Hz for different host accelerations. We attributed this striking result to the dissymmetrical atomic configuration of wurtzite ZnO, in which Zn^{2+} cations and O^{2-} anions exchange their position under the influence of external load heterogeneously. Simply, the voltage and electrical power output of $LiNbO_3$, AlN and ZnO cantilevers were found to increase linearly with the host acceleration.

Examination of electric properties of different cantilevers assembled on the three different substrates as a function of frequency indicates that the voltage, mechanical power input and electrical power output of all possible combinations of cantilever/substrate changes linearly with frequency. Among all the cantilever/substrate structures studied as a function of frequency, we found that the resonant frequency of ZnO cantilever assembled on aluminum, steel, and silicon substrates to be 173.5 Hz, 170 Hz and 175 Hz, respectively. When examined as a function of host acceleration, our results indicate that ZnO cantilever assembled on steel substrate at resonant frequency of 170 Hz attains maximum voltage and electrical power output of 9.83 V and 4.02 mW, respectively. We hope that our results on different cantilevers investigated in this study could improve the cantilevers applications ranging from aircraft design to architecture, medical diagnostics, nanoscale measurement systems, and forensics.

Conflicts of Interest

The authors declare no conflicts of interest regarding the publication of this paper.

References

[1] Sharma, S.R. and Pant, B. (2017) Design and Development of Guided Four Beam Cantilever Type MEMS Based Piezoelectric Energy Harvester. *Microsystem Technologies*, **23**, 1751-1759. https://doi.org/10.1007/s00542-016-2940-1

[2] Firoozy, P., Khadem, S.E. and Pourkiaee, S.M. (2017) Power Enhancement of Broadband Piezoelectric Energy Harvesting Using a Proof Mass and Nonlinearities in Curvature and Inertia. *International Journal of Mechanical Sciences*, **133**, 227-239. https://doi.org/10.1016/j.ijmecsci.2017.08.048

[3] Sun, S. and Peter, W. (2019) Modeling of a Horizontal Asymmetric U-Shaped Vibration-Based Piezoelectric Energy Harvester (U-VPEH). *Mechanical Systems and Signal Processing*, **114**, 467-485. https://doi.org/10.1016/j.ymssp.2018.05.029

[4] Wei, C. and Jing, X. (2017) A Comprehensive Review on Vibration Energy Harvesting: Modelling and Realization. *Renewable and Sustainable Energy Reviews*, **74**, 1-18. https://doi.org/10.1016/j.rser.2017.01.073

[5] Ahmed, R., Mir, F. and Banerjee, S. (2017) A Review on Energy Harvesting Approaches for Renewable Energies from Ambient Vibrations and Acoustic Waves Using Piezoelectricity. *Smart Materials and Structures*, **26**, Article ID: 085031. https://doi.org/10.1088/1361-665X/aa7bfb

[6] Toprak, A. and Tigli, O. (2018) Micron Scale Energy Harvesters Using Multiple Piezoelectric Polymer Layers. *Sensors and Actuators A*: *Physical*, **269**, 412-418. https://doi.org/10.1016/j.sna.2017.11.035

[7] Xiang, H.-J., Zhang, Z.-W., Shi, Z.-F. and Li, H. (2018) Reduced-Order Modeling of Piezoelectric Energy Harvesters with Nonlinear Circuits under Complex Conditions. *Smart Materials and Structures*, **2**, Article ID: 045004. https://doi.org/10.1088/1361-665X/aaaf92

[8] Tang, G., Yang, B., Liu, J.-Q., Xu, B., Zhu, H.-Y. and Yang, C.-S. (2014) Development of High Performance Piezoelectric d33 Mode MEMs Vibration Energy Harvester Based on PMN-PT Single Crystal Thick Film. *Sensors and Actuators A*: *Physical*, **205**, 150-155. https://doi.org/10.1016/j.sna.2013.11.007

[9] Elvin, N. and Erturk, A. (2013) Advances in Energy Harvesting Methods. Springer Science & Business Media, Berlin. https://doi.org/10.1007/978-1-4614-5705-3

[10] Du, S., Jia, Y., Do, C.D. and Seshia, A.A. (2016) An Efficient SSHI Interface with Increased Input Range for Piezoelectric Energy Harvesting under Variable Conditions. *IEEE Journal of Solid-State Circuits*, **51**, 2729-2742. https://doi.org/10.1109/JSSC.2016.2594943

[11] Han, M., Yuan, Q., Sun, X. and Zhang, H. (2014) Design and Fabrication of Integrated Magnetic MEMS Energy Harvester for Low Frequency Applications. *Journal of Microelectromechanical Systems*, **23**, 204-212. https://doi.org/10.1109/JMEMS.2013.2267773

[12] Körner, C., Bauereiß, A. and Attar, E. (2013) Fundamental Consolidation Mechanisms during Selective Beam Melting of Powders. *Modelling and Simulation in Materials Science and Engineering*, **21**, Article ID: 085011. https://doi.org/10.1088/0965-0393/21/8/085011

[13] Lee, K. and Fishwick, P.A. (2001) Building a Model for Real-Time Simulation. *Future Generation Computer Systems*, **17**, 585-600. https://doi.org/10.1016/j.vacuum.2004.01.052

[14] http://www.comsol.com

[15] Akiyama, M., Nagao, K., Ueno, N., Tateyama, H. and Yamada, T. (2004) Influence

of Metal Electrodes on Crystal Orientation of Aluminum Nitride Thin Films. *Vacuum*, **74**, 699-703. https://doi.org/10.1016/j.vacuum.2004.01.052

[16] Shampa, M. (2014) Preparation of Undoped and Some Doped ZnO Thin Films by Silar and Their Characterization. Bardhaman, New York.

[17] Mackwitz, P., Rüsing, M., Berth, G., Widhalm, A., Müller, K. and Zrenner, A. (2016) Periodic Domain Inversion in X-Cut Single-Crystal Lithium Niobate Thin Film. *Applied Physics Letters*, **108**, Article ID: 152902. https://doi.org/10.1063/1.4946010

[18] Elfrink, R., Kamel, T., Goedbloed, M., Matova, S., Hohlfeld, D., Van Andel, Y., *et al*. (2009) Vibration Energy Harvesting with Aluminum Nitride-Based Piezoelectric Devices. *Journal of Micromechanics and Microengineering*, **19**, Article ID: 094005. https://doi.org/10.1088/0960-1317/19/9/094005

[19] Zhao, X., Shang, Z., Luo, G. and Deng, L. (2015) A Vibration Energy Harvester Using AlN Piezoelectric Cantilever Array. *Microelectronic Engineering*, **142**, 47-51. https://doi.org/10.1016/j.mee.2015.07.006

[20] Battista, L., Mecozzi, L., Coppola, S., Vespini, V., Grilli, S. and Ferraro, P. (2014) Graphene and Carbon Black Nano-Composite Polymer Absorbers for a Pyro-Electric Solar Energy Harvesting Device Based on $LiNbO_3$ Crystals. *Applied Energy*, **136**, 357-362. https://doi.org/10.1016/j.apenergy.2014.09.035

[21] Kumar, B. and Kim, S.-W. (2012) Energy Harvesting Based on Semiconducting Piezoelectric ZnO Nanostructures. *Nano Energy*, **1**, 342-355. https://doi.org/10.1016/j.nanoen.2012.02.001

[22] Song, J., Zhou, J. and Wang, Z.L. (2006) Piezoelectric and Semiconducting Coupled Power Generating Process of a Single ZnO Belt/Wire. A Technology for Harvesting Electricity from the Environment. *Nano Letters*, **6**, 1656-1662. https://doi.org/10.1021/nl060820v

[23] Mahmud, A., Khan, A.A., Voss, P., Das, T., Abdel-Rahman, E. and Ban, D. (2018) A High Performance and Consolidated Piezoelectric Energy Harvester Based on 1D/2D Hybrid Zinc Oxide Nanostructures. *Advanced Materials Interfaces*, **5**, Article ID: 1801167. https://doi.org/10.1002/admi.201801167

[24] Erturk, A. and Inman, D.J. (2008) On Mechanical Modeling of Cantilevered Piezoelectric Vibration Energy Harvesters. *Journal of Intelligent Material Systems and Structures*, **19**, 1311-1325. https://doi.org/10.1177/1045389X07085639

[25] Kumari, K. and Khanna, G. (2016) Design and Simulation of Array of Rectangular Micro Cantilevers Piezoelectric Energy Harvester. *International Journal of Engineering Research and Applications*, **6**, 41-49.

[26] Anton, S. and Sodano, H.A. (2007) A Review of Power Harvesting Using Piezoelectric Materials (2003-2006). *Smart Materials and Structures*, **16**, R1-R21. https://doi.org/10.1088/0964-1726/16/3/R01

[27] Wang, Z.L. and Song, J. (2006) Piezoelectric Nanogenerators Based on Zinc Oxide Nanowire Arrays. *Science*, **312**, 242-246. https://doi.org/10.1126/science.1124005

[28] Pan, Z.W., Dai, Z.R. and Wang, Z.L. (2001) Nanobelts of Semiconducting Oxides. *Science*, **291**, 1947-1949. https://doi.org/10.1126/science.1058120

[29] Hu, G., Ma, Y. and Wang, B. (2009) Mechanical Properties and Morphology of Nylon 11/Tetrapod-Shaped Zinc Oxide Whisker Composite. *Materials Science and Engineering A*, **504**, 8-12. https://doi.org/10.1016/j.msea.2008.12.025

[30] https://www.memsnet.org/material/aluminumnitridealnbulk/

[31] https://www.korth.de/index.php/162/items/19.html

[32] Nann, T. and Schneider, J. (2004) Origin of Permanent Electric Dipole Moments in Wurtzite Nanocrystals. *Chemical Physics Letters*, **384**, 150-152. https://doi.org/10.1016/j.cplett.2003.12.017

[33] Anota, E.C., Villanueva, M.S. and Cocoletzi, H.H. (2010) Electronic Properties of Group III: A Nitride Sheets by Molecular Simulation. *Physica Status Solidi C*, **7**, 2252-2254. https://doi.org/10.1002/pssc.200983499

[34] Maggard, P.A., Nault, T.S., Stern, C.L. and Poeppelmeier, K.R. (2003) Alignment of Acentric MoO_3F_{33}-Anions in a Polar Material: $(Ag_3MoO_3F_3)(Ag_3MoO_4)$ Cl. *Journal of Solid State Chemistry*, **175**, 27-33. https://doi.org/10.1016/S0022-4596(03)00090-2

[35] Reilly, E.K., Burghardt, F., Fain, R. and Wright, P. (2011) Powering a Wireless Sensor Node with a Vibration-Driven Piezoelectric Energy Harvester. *Smart Materials and Structures*, **20**, Article ID: 125006. https://doi.org/10.1088/0964-1726/20/12/125006

[36] Pan, C., Liu, Z., Chen, Y. and Liu, C. (2010) Design and Fabrication of Flexible Piezo-Microgenerator by Depositing ZnO Thin Films on PET Substrates. *Sensors and Actuators A*: *Physical*, **159**, 96-104. https://doi.org/10.1016/j.sna.2010.02.023